

3 Structural design assisted by wind tunnel testing

Massimo Majowiecki, Nicola Cosentino
Università IUAV di Venezia

3.1 INTRODUCTION

This Chapter presents some of the recent experiences in wind tunnel testing, made by the Authors within the design stage of steel structures. According to principle of the «design assisted by testing», contemplated by the Eurocode, the combination of tests and calculations is increasingly used. Multiples are the motivation of this increasing interest/demand. The sophisticated architectural shapes (culminating in the «free form design»), the absence of corresponding reliable fluid-dynamics models and the increasing flexibility of structures are probably the main ones. Not less important is the opportunity/necessity to confirm by control checks the assumptions made in the design, specially with respect to complex aeroelastic phenomena, such as lock-in, flutter, rain-wind induced vibration, etc..

The main purpose of the paper is to outline the potentiality of the presented tests and the main problems encountered in their use. These aspects have to be accurately evaluated in defining the test specifications.

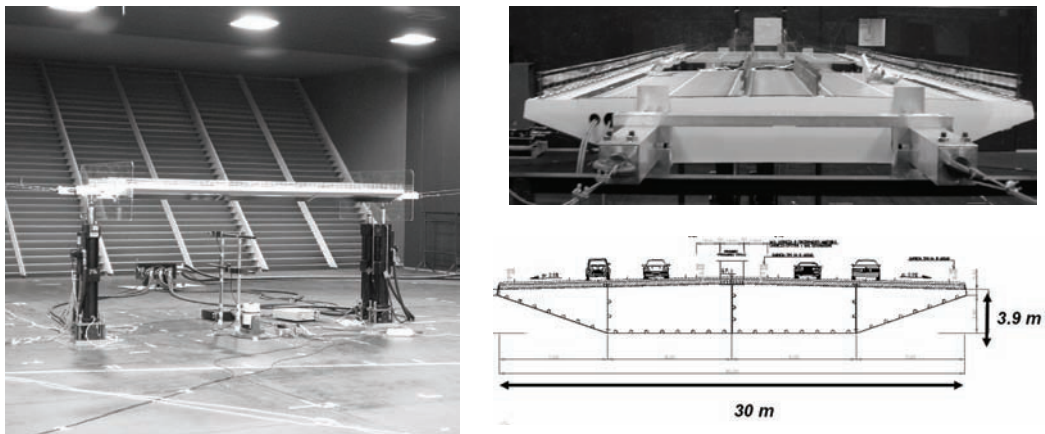


Figure 3.1 Experimental deck model and deck section (Adige River Bridge)

The use of some data analysis techniques (such as the proper orthogonal decomposition, the sensitivity analysis, etc.), in keeping the essential design parameters, is presented too.

The presented experiences refer to the tests performed during the design of: a cable stayed bridge on the Adige river (on the A31 motorway - Italy); the New Braga Stadium (Braga - Portugal); the new Unipol headquarter Tower (Bologna - Italy); the tall building and the roof on «Piazza delle Città Lombarde» (Milan - Italy); the new Bologna town-hall (Bologna - Italy).

3.2 THE ADIGE RIVER BRIDGE

The design of the Adige river cable stayed bridge [1] was assisted by wind tunnel tests aimed to check the aerodynamic and the aeroelastic behaviour of the deck and of the tower. The tests were carried out at the «Politecnico di Milano» boundary layer wind tunnel (Fig. 3.1).

Regarding the bridge deck, the aerodynamic static coefficients and the flutter derivatives (with a particular focus on the low reduced velocity values) were measured. The bridge deck was modeled by an elastic mockup made by an aluminum structure. Since the (expected) ratio between the flexural and the torsional frequencies was quite close to the unity (0.85), this ratio was reproduced at the model scale to correctly take it into account for flutter investigation.

The quasi-steady aerodynamic forces were measured in low turbulence conditions, at different angles of attack. The aerodynamic coefficients (Fig. 3.2) allow to determine the quasi-steady wind forces on the deck and to check the sensitivity to galloping.

The aeroelastic behaviour was investigated by both a direct and an inverse method. By the direct method the wind induced forces on the deck, under an imposed 1-DOF motion, are measured.

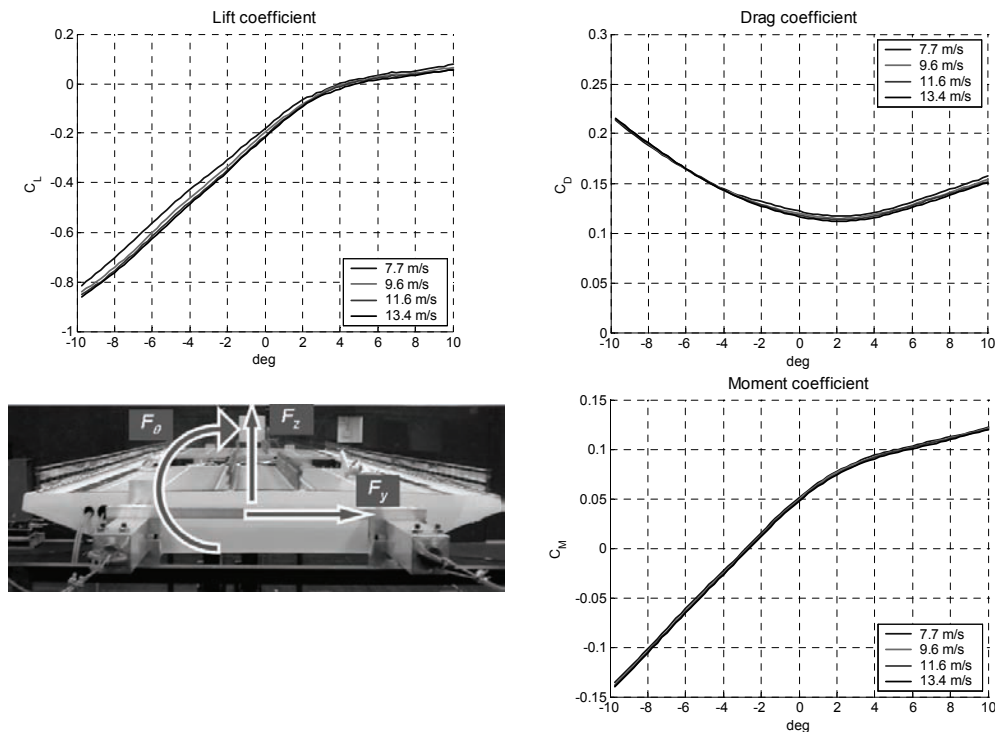


Figure 3.2 The aerodynamic static coefficients and their sign convention

This allows to define and change a-priori the (mean) angle of attack; it also allows a large reproducibility of the tests. On the other hand, the inverse method consist in measuring the forces on the duck during a free motion. This procedure allows to investigate the vortex shedding mechanism.

Based on the wind tunnel measured aeroelastic derivatives (Fig. 3.3), the flutter critical conditions (velocity and frequency) have been investigated by mean of the classical Scanlan-Tomko procedure (Fig. 3.4). The order of magnitudes have been checked by comparing the results with those obtained by the simplified Theodorsen theory. The influence of the angle of attack and of the inherent structural damping on the critical parameters has been checked too.

In order to keep the aeroelastic behaviour at very low wind speeds, an alternative approach to the flutter problem has been adopted. The aerodynamic forces are written as:

$$\begin{aligned}
 F_z &= \frac{1}{2} \rho V^2 BL \left(-h_1^* \frac{\dot{z}}{V} - h_2^* \frac{B \dot{\vartheta}}{V} + h_3^* \vartheta + h_4^* \frac{\pi}{2V_\omega^{*2}} \frac{z}{B} \right) \\
 F_\vartheta &= \frac{1}{2} \rho V^2 B^2 L \left(-a_1^* \frac{\dot{z}}{V} - a_2^* \frac{B \dot{\vartheta}}{V} + a_3^* \vartheta + a_4^* \frac{\pi}{2V_\omega^{*2}} \frac{z}{B} \right)
 \end{aligned}
 \tag{3.1}$$

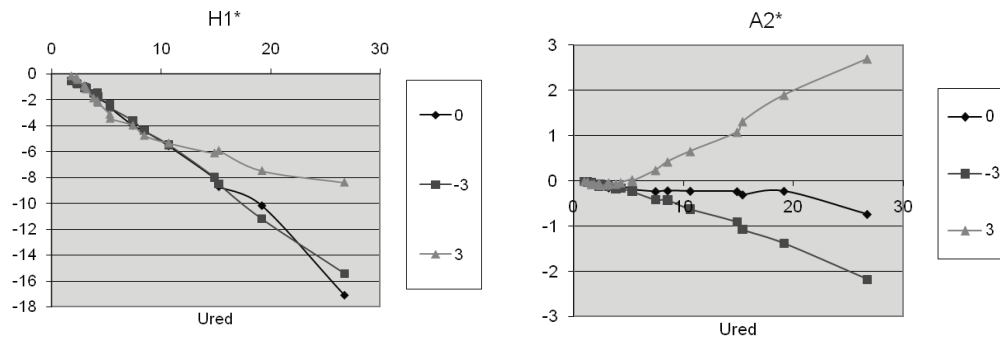


Figure 3.3 Flutter derivatives $H1^*$ and $A2^*$, for the attack angles 0° , 3° , -3°

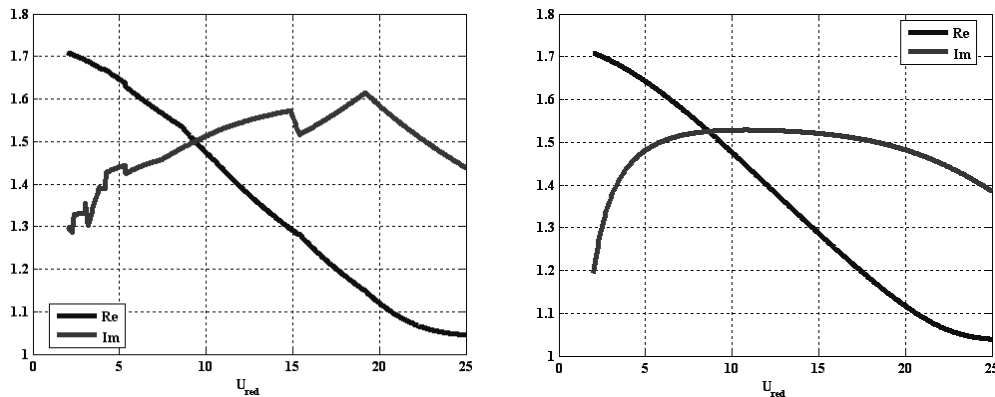


Figure 3.4 Real and imaginary parts of the flutter equation solution. Coupling of modes 1 and 3 – angle of attack 0° - linear interpolation (left) vs polynomial fitting of experimental coefficients (right)

where B and L are the deck dimensions ($L = \text{unit length}$), ρ is the air density, V is the wind speed, $V^*_\omega = V/\omega B$ is the reduced velocity, ω is the angular frequency, θ and z are the deck DOFs. It is possible to calculate the minimum damping necessary to avoid the excitation due to vortex shedding. By considering only the equation of motion for the vertical displacement (which, in the present case, corresponds to the first vibration mode), the total damping is obtained by the superposition of aeroelastic and structural damping components.

In order to obtain stability against vortex-shedding, the total damping must be positive (Fig. 3.5):

$$\xi \geq -\frac{\rho V^* B^2 h_1^*}{8m\pi} \tag{3.2}$$

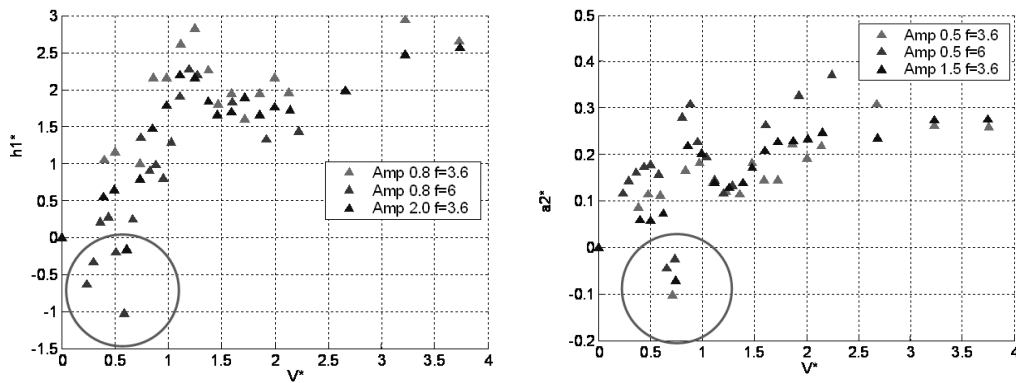


Figure 3.5 Flutter derivatives $h1^*$ and $a2^*$, at low reduced velocity

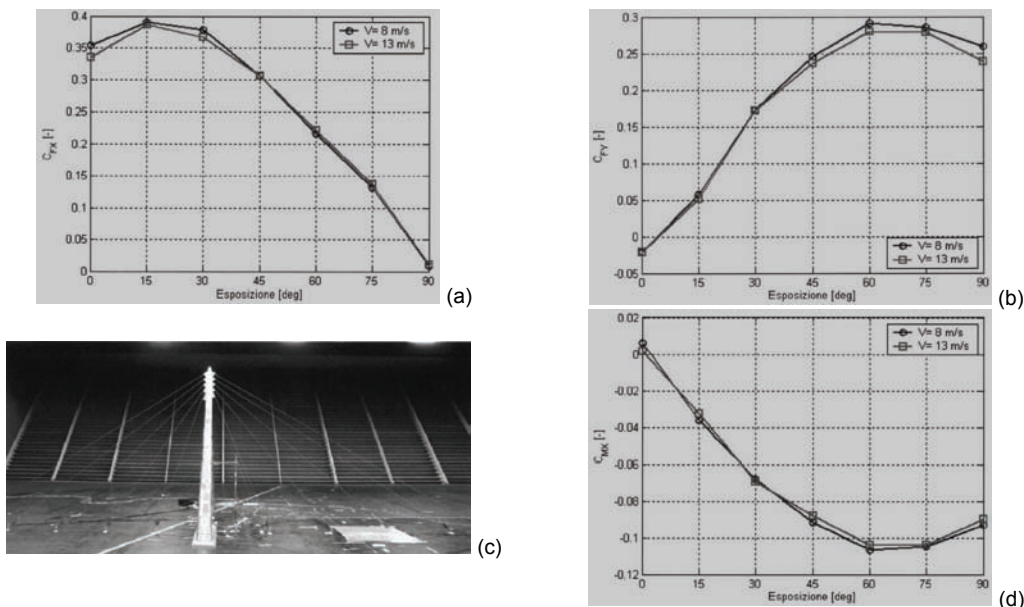


Figure 3.6 Aerodynamic coefficients at the pylon base: (a) C_{FX} , (b) C_{FY} , (d) C_{MX}

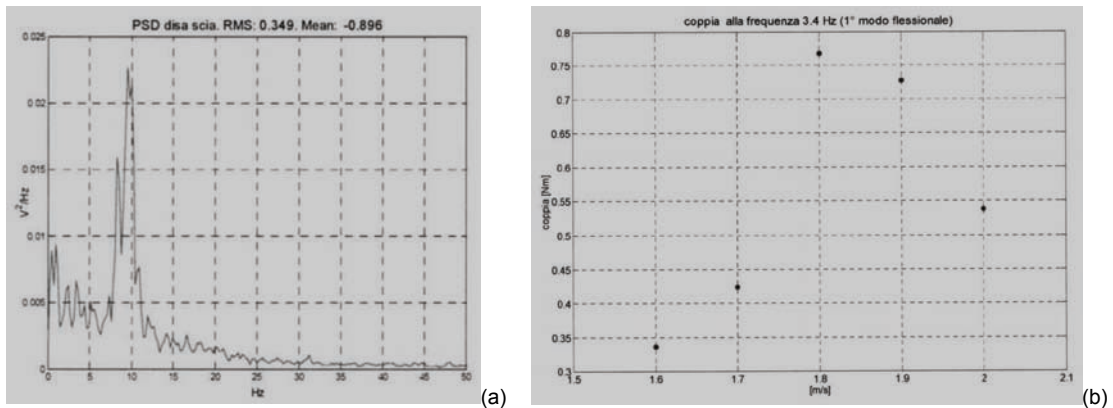


Figure 3.7 Spectral properties of the wake (a) and base bending moment vs wind speed (b)

V^* being the reduced velocity $V^* = V / Bf$. Of course, this is an approximate procedure, because vortex shedding is a strongly non-linear phenomenon; it is here treated by a linear approach, but this allows to estimate the order of magnitude for the minimum structural damping which is necessary to protect the structure from vortex-shedding.

The bridge tower model (flexible aeroelastic model) was firstly placed on a dynamometric balance to determine the aerodynamic forces and moments (Fig. 3.6) due to smooth wind. The same model was then linked to the ground and equipped by accelerometers and extensometers to measure the vibration induced by the vortex shedding. An independent anemometer measured the wake wind speed.

The aerodynamic forces are used in the design of the tower sections. The “in-wake” wind velocity spectra (Fig. 3.7a) allow to determine the Strouhal number; the relatively low dynamic magnification factor (DMF) of the bending moment (in the pylon) at the lock-in velocity (Fig. 3.7b) shows a moderate sensitivity to vortex shedding.

3.3 THE NEW BRAGA STADIUM

The tests for the design of the new Braga Stadium suspended roof [2-7] were carried out, independently, at the “RWDI” and at the “Politecnico di Milano” wind tunnels. “RWDI” tests were performed on rigid models, to measure the pressure field on the roof, while a flexible (aeroelastic) model was tested at the “Politecnico di Milano”, in order to check the aerodynamic stabilities and the effectiveness of a possible external damping system.

The wind pressures were derived from the tests on a rigid model (Fig. 3.8). Since the pressure time histories were simultaneously measured at different points, within the upper and the lower sides of the roof panels, the instantaneous pressure fields were available.

Due to the different spatial distribution of upper and lower pressure taps, preliminary interpolation was required to obtain the differential pressures, which represent the actual load on the structure. Despite the apparent simplicity of this operation, the instantaneous interpolation gave rise to uncertainties and numerical difficulties.

The design wind speeds at the stadium site were derived from 1:1500 scaled wind tunnel tests (including a wide stadium surroundings), while the pressure coefficients were measured in 1:400 model.

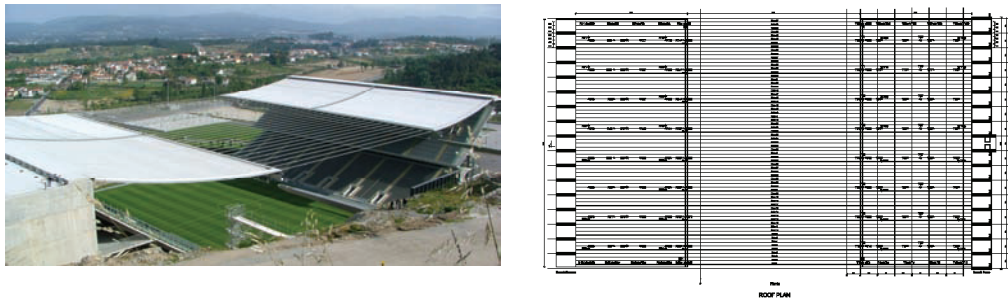


Figure 3.8 The New Braga Stadium and the RWDI pressure taps arrangement

Both the wind speed profiles and turbulence presented different features in 1:400 tests with respect to 1:1500 ones. In order to match the peak gust velocities between the two scale models at 25 and 50 m heights (roof position), an equivalent design wind speed was calculated by RWDI. The “double model” was a source of further uncertainties and data treatment problems. It also outlined a more general problem which often occurs in defining the model reference height: due to the imperfect reproduction of the wind profile, significant errors can befall when wind tunnel dimensionless coefficients are used with reference to standard codes design wind speed.

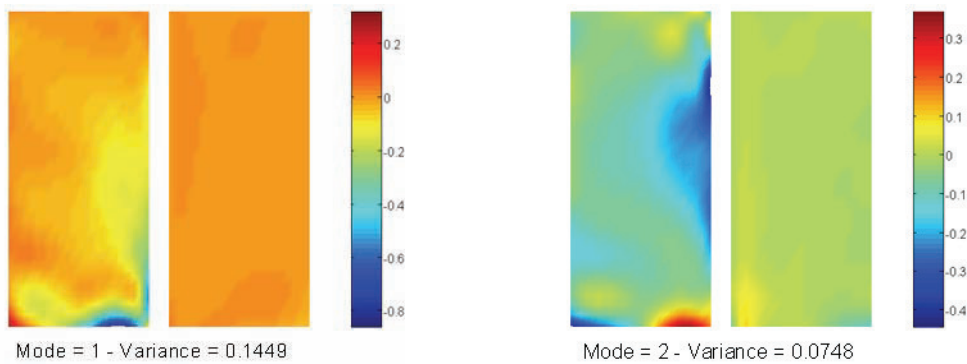


Figure 3.9 Proper orthogonal decomposition of the measured wind pressure fields

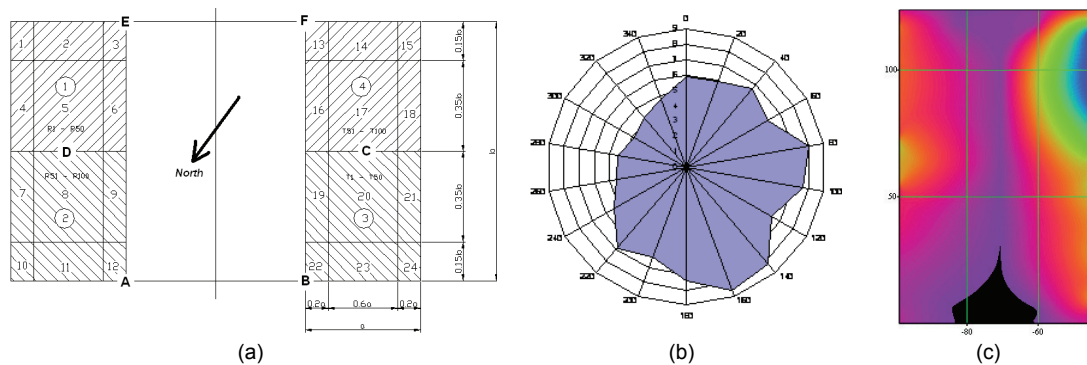


Figure 3.10 References points/regions for the response evaluation and the sensitivity analysis (a), minimum reliability index β for each direction (b) and distribution of β values along the slab (c)

The orthogonal decomposition techniques have been adopted to simplify the pressure representation, and to reduce the computational effort. The structural response was determined by separately evaluating the mean, the quasi-steady and the resonant response. The first term simply takes into account the mean pressure distributions. The second one is obtained by performing a classical covariance proper orthogonal decomposition (POD). The third one takes into account the dynamic amplification of a suitable number of structural vibration modes, each one being excited by the unsteady wind pressures.

The analytical procedure is synthesized in the following equations, while a typical result is summarized in Table 3.1 (with the reference to Fig. 3.10a). The Eqs. (3.3) resume the procedure to decompose (POD) a pressure field (Fig. 3.9), the Eqs. (3.4) determine the mean and the quasi-static response and the Eqs. (3.5) refer to the resonant contribution.

Let $\mathbf{p}(t) = \{p_1(t) \dots p_m(t)\}^T$ be a Gaussian stationary nil mean m -variate random process. Let \mathbf{C}_p be the covariance (for $\tau = 0$) matrix of $\mathbf{p}(t)$. This matrix is symmetric and positive definite, thus it admits the modal decomposition:

$$\mathbf{C}_p = \sum_{k=1}^m \phi_k \phi_k^T \lambda_k; \quad \phi_i \phi_j^T = \delta_{ij}; \quad \phi_i^T \mathbf{C}_p \phi_j = \delta_{ij} \lambda_j; \quad \mathbf{p}(t) = \sum_{k=1}^m \phi_k x_k(t) \quad (3.3)$$

where λ_k and ϕ_k are k^{th} eigenvalue and eigenvector of \mathbf{C}_p and $\mathbf{x}(t) = \{x_1(t) \dots x_m(t)\}^T$ is the m -variate random process, image of $\mathbf{p}(t)$ in the transformed space.

The generic response $R(t)$ of a linear system to the load $\mathbf{p}(t)$ can be expressed as:

$$R(t) = \sum_{k=1}^s x_k(t) \cdot R_k; \quad \sigma_{R,qs}^2 = \sum_{k=1}^s \sigma_{x_k}^2 R_k^2; \quad R_{qs} = \bar{R} \pm g_{qs} \sigma_{R,qs} \quad (3.4)$$

where R_k is the generic response (load, deflection, etc.) due to the static distribution ϕ_k ; $\sigma_{x_k}^2$ is the variance of the process $x_k(t)$; g_{qs} is the quasi-steady gust factor; $\sigma_{R,qs}$ is the standard deviation of R ; R_{qs} is the quasi-steady peak (minimum and maximum) response.

The inclusion of resonant effects can be accomplished using the equations:

$$R_{qs+res} = \bar{R} \pm \sqrt{g_{qs}^2 \sigma_{R,qs}^2 + g_{res}^2 \sigma_{R,res}^2}; \quad g_{res}^2 \sigma_{R,res}^2 = \sum_{h=1}^n g_h^2 \sigma_{R_h}^2$$

$$g_h = \sqrt{2 \ln(f_h T)} + \frac{0.577}{\sqrt{2 \ln(f_h T)}}; \quad M_h = \int_A m(x, y) \cdot \psi_h^2(x, y) \cdot dA \quad (3.5)$$

$$Q_h(t) = \int_A p(x, y, t) \cdot \psi_h(x, y) \cdot dA; \quad \sigma_{R_h}^2 = R_h^2 \frac{\pi}{4 \cdot \xi_h} \frac{f_h \cdot S_{Q_h}(f_h)}{(2 \cdot \pi \cdot f_h)^4 M_h^2}$$

where g_h is the h^{th} modal gust factor; f_h is the natural frequency of the h^{th} mode; T is the sample length (typically one hour); $\sigma_{R_h}^2$ is the variance of response R associated to the mode h ; $\psi_h(x, y)$ is the h^{th} mode shape, in terms of deflection normal to the surface at the position (x, y) ; R_h is the response corresponding to this deflection; $m(x, y)$ is the mass per unit area; ξ_h is the h^{th} modal damping; $S_{Q_h}(f)$ is the modal force spectrum.

The resonant contribution is proportional to the square of the inherent structural damping ratio. Since this contribute was the most important in the case of the Braga Stadium (see Table 3.1), a

more appropriate evaluation of the structural damping was necessary (full scale dynamic characterization) and an experimental check of the resonant and aeroelastic effects was made (aeroelastic model).

The aeroelastic model (1:70) was tested at the “Politecnico di Milano” boundary layer wind tunnel (BLWT) in both smooth flow (without external environmental reconstruction) and turbulent flow (with external environmental reconstruction). The aeroelastic stability was checked up to 58 m/s (full scale). In turbulent wind conditions, oscillation up to 40-50 cm full scale, as order of magnitude, were recorded. The aeroelastic model was also tested by placing (at the roof corners) linear viscous dissipative devices ($C = 100-150$ kN s/m at full scale). Damping ratios up to 7-8% were reached. The response was subsequently reduced of about 50%, so confirming the analytical estimations.

In January 2004 the structure was equipped with a permanent monitoring system, to measure different parameters (such as pressures, accelerations, wind velocity, cable stresses, etc.) at different significant points of the structure (Fig. 3.11).

As it was found numerically and confirmed by the aeroelastic model, the resonant response is dominant and the structural inherent damping was a very important parameter in determining the response.

Node	\bar{R}	$\xi_{qs}^2 \sigma_{R,qs}^2$	$\bar{R} \pm \sqrt{\xi_{qs}^2 \sigma_{R,qs}^2}$	$\xi_{res}^2 \sigma_{R,res}^2$	$\bar{R} \pm \sqrt{\xi_{qs}^2 \sigma_{R,qs}^2 + \xi_{res}^2 \sigma_{R,res}^2}$
A	0,1550	0,0250	0,3131	0,3027	0,7275
B	-0,0837	0,0115	-0,1910	0,3076	-0,6486
C	-0,0441	0,0014	-0,0812	0,0433	-0,2555
D	0,0930	0,0052	0,1652	0,0419	0,3101
E	0,0621	0,0092	0,1582	0,2040	0,5238
F	-0,0198	0,0016	-0,0599	0,2018	-0,4709

Table 3.1 Typical response contributions, in terms of vertical displacement at some roof locations: mean (col. 2), quasi-static (col. 4) and total response (col. 6)



Figure 3.11 Monitoring system on the whole structure

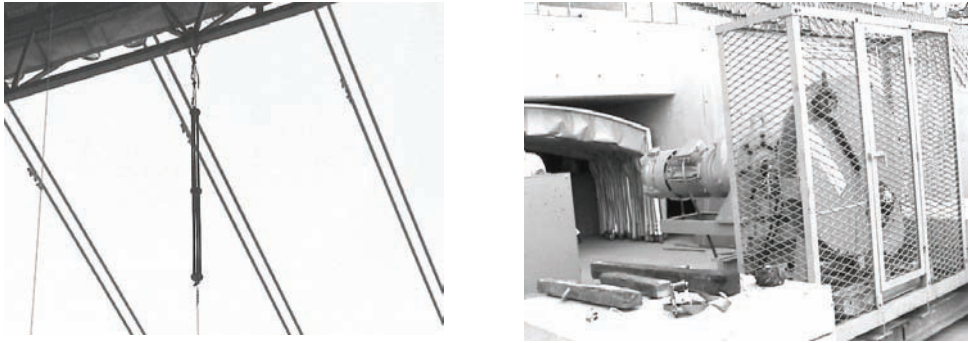


Figure 3.12 Images of the exciting system

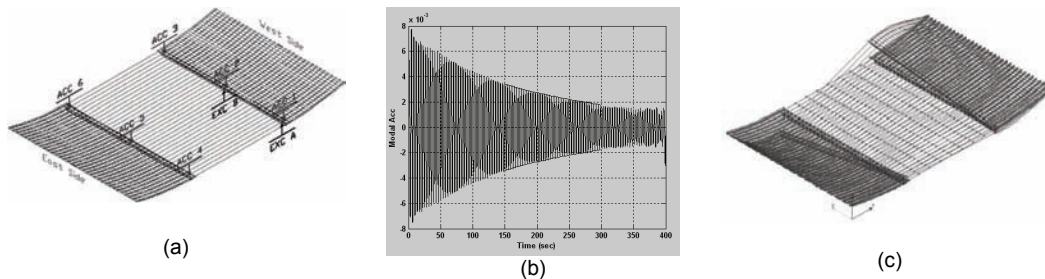


Figure 3.13 Exciting-measuring positions (a), typical free motion record (b) and 1st natural mode (c)

The dynamic characterization was performed to determine the actual value of the damping ratio for the first modes. To excite the system, a cable was attached to the border steel girder through a pre-tensioned spring (Fig. 3.12a) and it was harmonically moved (sinus wave) at the other end by an electrical engine (Fig. 3.12b). To measure the structural dynamic response under the applied dynamic loads and the free vibration decay after the loading excitation stop, 6 accelerometers were placed on the roof slab (Fig. 3.13a).

In order to evaluate the natural modal shapes and the corresponding modal damping, the free vibration decay time series, recorded after the resonant harmonic excitation stops, have been used (Fig. 3.13b). The modal shapes were determined by orthogonal decomposing (POD) the recorded signals (Fig. 3.13c).

3.4 THE UNIPOL TOWER

The design of the “Unipol” tall (123 m) building [8] was assisted by wind tunnel tests carried out at the CRIACIV¹ (Florence/Prato, Italy) boundary layer wind tunnel on a rigid model 1:350 scaled and equipped with 125 pressure taps (Fig. 3.14).

¹ Cento di Ricerca Interuniversitario di Aerodinamica delle Costruzioni e Ingegneria del Vento (Univ. di Firenze, Roma La Sapienza, Perugia, Trieste, Venezia IUAV, Chieti D’Annunzio); www.criaciv.unifi.it.

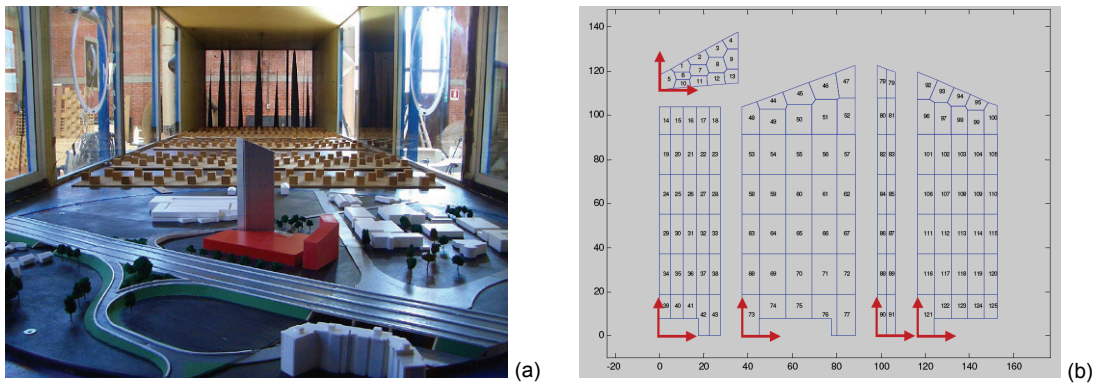


Figure 3.14 The Unipol Tower wind tunnel model (a) and the pressure taps locations (b)

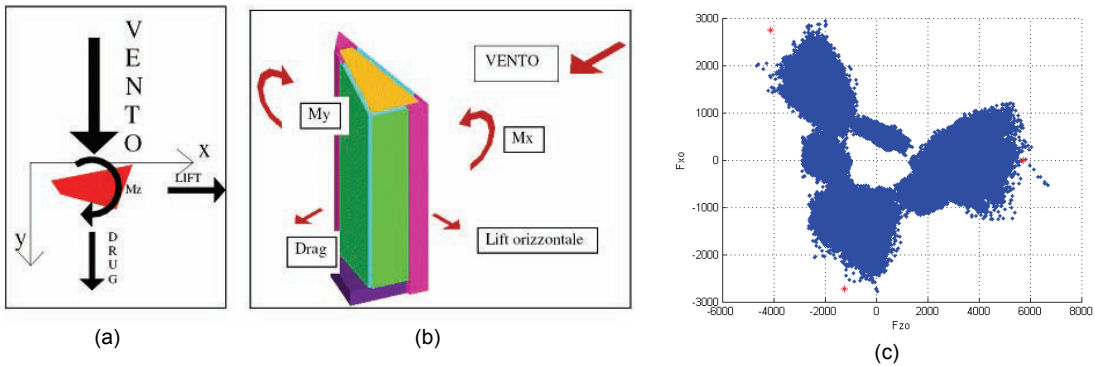


Figure 3.15 Wind tunnel reference system (a,b) and correlation locus of longitudinal-transversal force (c)

The aim of the tests was to determine the aerodynamic forces by both the simultaneous measurement of pressures at 125 points on the facades and the direct measurement of the base global forces by means of a dynamometric balance. In addition, pressures and flow within a double skin facade, which covers part of the building, were required to be checked.

Once the preliminary treatment and reliability problems were overcome, the simultaneous pressure fields were retained. The design forces on the building were evaluated at different levels, by taking into account the correlation between the components. Due to the asymmetry of the structure, the significant load combinations were determined by means of the longitudinal-transversal force locus (Fig. 3.15c), by including all the tested wind directions. In addition, information on local pressures were also available. The measurement of simultaneous pressure fields is quite “rich” of information, even if the comparison with directly measured global forces is suggested.

3.5 THE MILAN «ASRL»

The new Milan regional government centre (“Altra Sede Regione Lombardia” - ASRL) includes different steel structures: from the roof on the central place to parts of the tall main building.

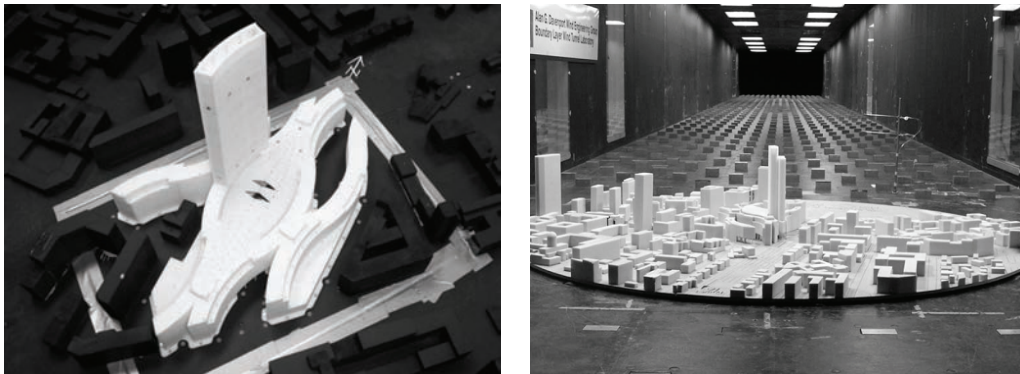


Figure 3.16 Wind tunnel model of the ASRL buildings and surrounding

The tests [9] were carried out at the “Alan G. Davenport Wind Engineering Group” BLWT (Fig. 3.16). Since the analysis included both the wind climate and the global design forces, this was a comprehensive wind tunnel study. In particular, the following informations were provided: (a) overall wind loads suitable for use in the design of the structural system of the tower; (b) local peak pressures acting on the external surfaces of the project; (c) local net peak pressures (external pressure minus internal pressure) suitable for use in the design of the windows and cladding; (d) load distributions for structural analysis of the Piazza roof; (e) prediction of the wind environment in pedestrian areas around the site; (f) smoke flow through the Piazza roof opening.

The resulting net pressure coefficients from the wind tunnel tests were combined with the design probability distribution of wind speed and direction to form predictions of net suction and pressures for various return periods (Fig. 3.17).

Regarding the Piazza Roof, five different structural load cases were considered and arranged by means of the measured pressure time histories at 107 locations. The load cases arrangement was oriented to maximize the overturning moments about edge lines of the roof as well as the center line of the roof, the shear in the x direction and uplift in the z direction (Fig. 3.18). Predictions of the load cases were made by combining the angle-by-angle aerodynamic data with the Milan wind climate model.

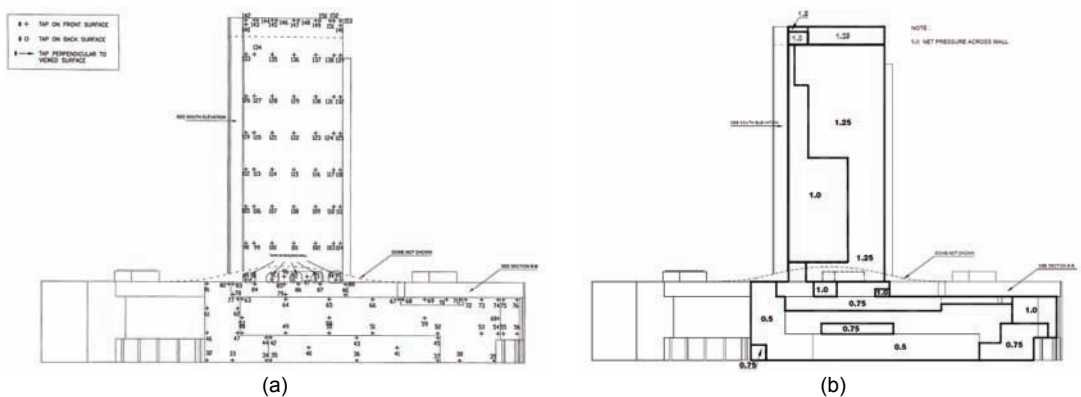


Figure 3.17 Example of pressure taps location on the Tower (a) and pressure distribution (b)

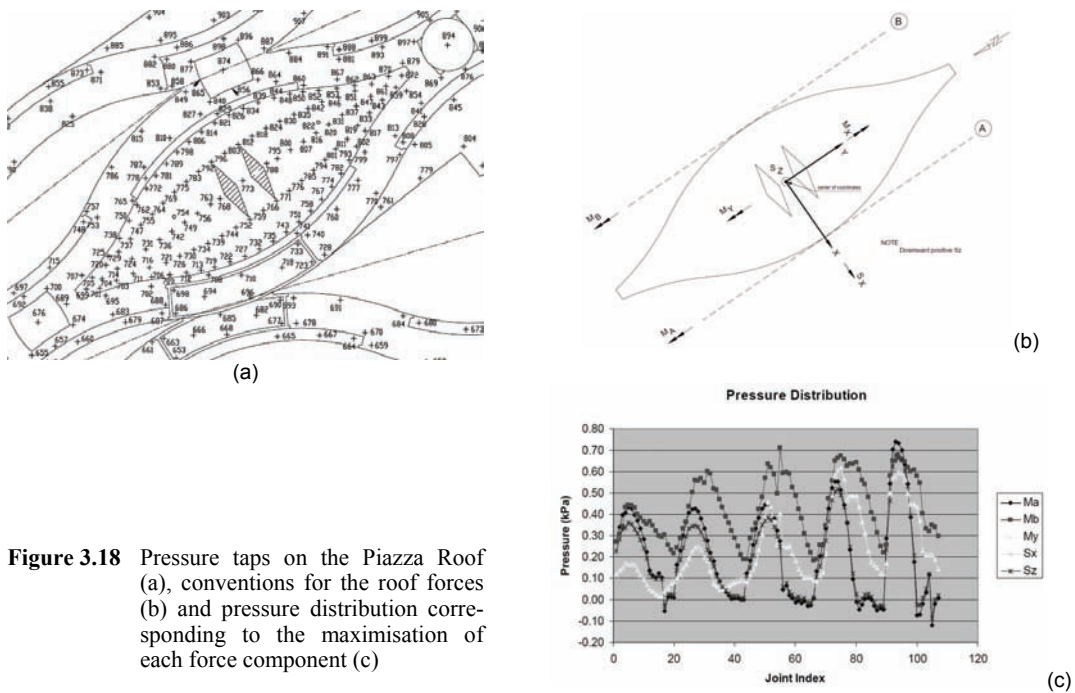


Figure 3.18 Pressure taps on the Piazza Roof (a), conventions for the roof forces (b) and pressure distribution corresponding to the maximisation of each force component (c)

Equivalent static loads were determined by using the load-response-correlation (LRC) method, based on the influence function for the load action and the correlation of the measured pressure data.

Fig. 3.19a shows the locations where pedestrian level wind speeds were measured. Experimental results were combined with the extratropical wind climates to provide predictions of the wind speeds expected to be exceeded for 5% of the time and those expected to be exceeded once per year. These predictions were compared directly with acceptance criteria for pedestrian comfort and safety, respectively (Fig 19b,c).

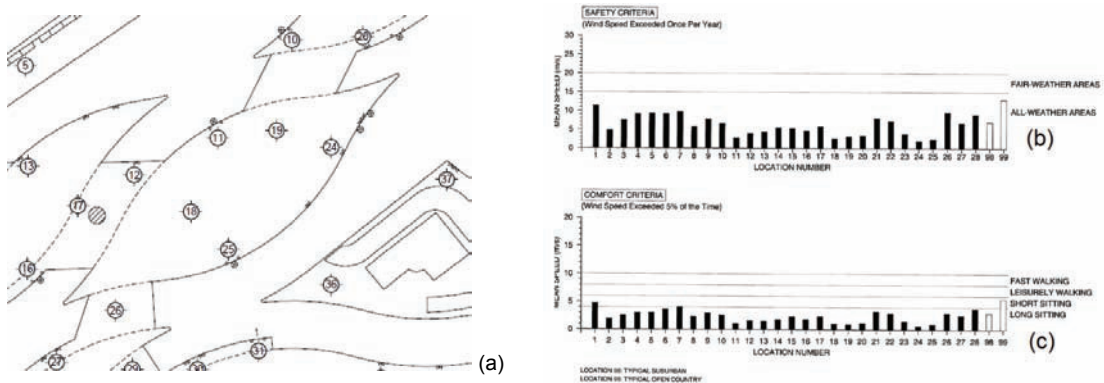


Figure 3.19 Location of measurements (a) and predicted mean wind speeds compared with criteria for pedestrian safety (b) and comfort (c)

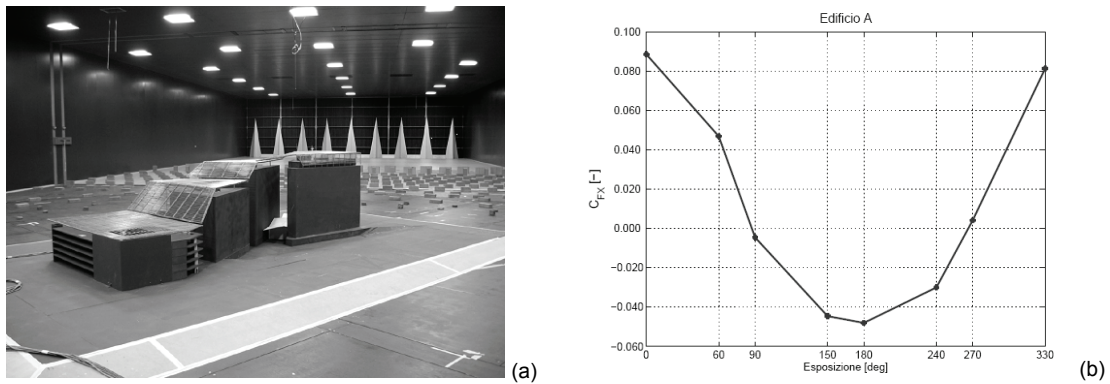


Figure 3.20 Bologna Town Hall model (a) and a typical force coefficients diagram on the roof (b)

Finally, the effectiveness of the Piazza roof opening to allow smoke to escape was determined by the plume rise height of the smoke generated in the open space underneath the roof. Analytical calculations of the plume rise were carried out for low wind conditions as well as nominal one week return and one month return wind speeds. The results suggest that the plume rise heights are much larger than the height of the Piazza roof from the ground and the smoke generated in a fire can likely escape the enclosure.

3.6 BOLOGNA TOWN HALL

The Bologna town hall structural design was assisted by wind tunnel tests performed at the “Politecnico di Milano” BLWT [10,11]. Two different models were arranged: a 1:50 model of the whole structure (Fig. 3.20a), for the measurement of loads on roofs and facades; a 1:1 model of a roof tube array (Fig. 3.22), to check the sensitivity to vortex shedding.

The 1:50 model of the whole structure was used to measure the forces on the roof (by means of dynamometric balances) and the pressures on facades (by means of appropriate distribution of pressure taps).

Loads on the roofs were given in terms of force coefficients (Fig. 3.20b), while pressures on facades were given in terms of pressure coefficient diagrams (Fig. 3.21a,b) and global maps (Fig. 3.21c).

The building roof is covered by a series of tube arrays, regularly spaced. The length of tubes varies between 7 and 14 m. The length-diameter ratio (up to 39), the light weight (aluminum) and the end connection type (which produces a very low damping ratio, approximately $\xi = 0.2\%$) make the tubes susceptible of dynamic excitation. Since the Scruton number is approximately 2.3, it is expected that the tubes are sensitive to vortex shedding excitation.

In the case of isolated cylinder, this Scruton number value gives rise to oscillations of about 0.3 diameters. The array effect is also tested in the wind tunnel (Fig. 3.22). The results substantially confirm the provisions made for the single tube, the recorded displacement being 0.25 diameters as order of magnitude.

Wind tunnel tests showed that the tube oscillation can reach amplitudes which can induce damage on the tubes themselves and on the connection, as well as appreciable oscillation of the whole roof. In addition, the “look-in” velocity (Fig. 3.23) corresponds to mean wind speed characterized by a low return period.

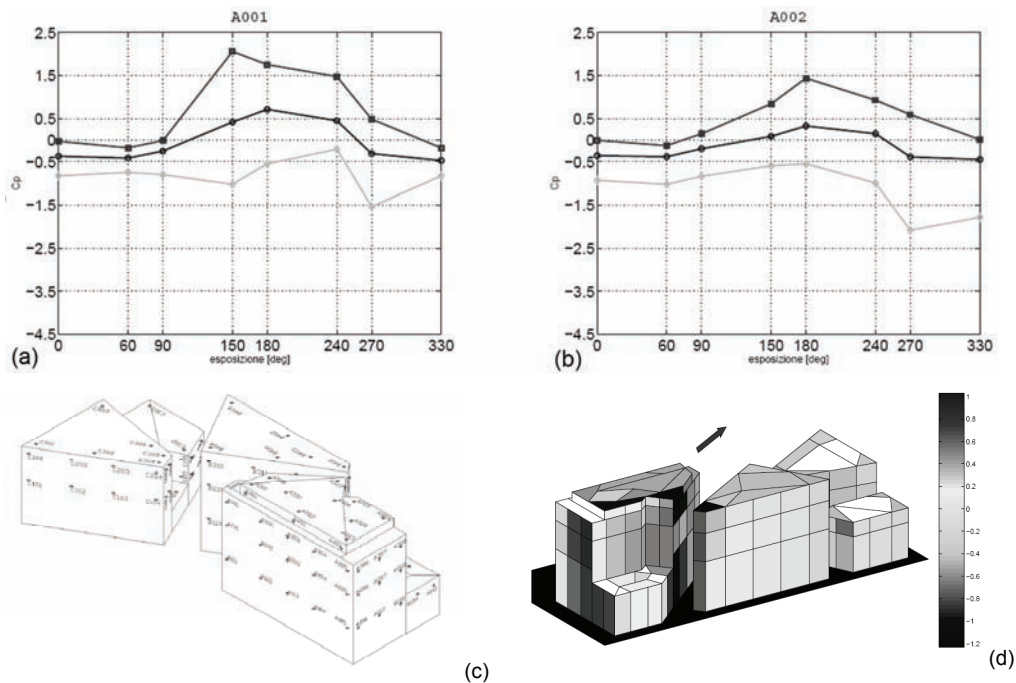


Figure 3.21 Typical pressure coefficients on facades (a,b), pressure taps location (c) and typical pressure map (d) for the Bologna Town Hall

Wind tunnel tests suggested to implement design solution to avoid or reduce the sensitivity to vortex shedding. Possible ways to do so are aerodynamic solutions (such as placing spires on the tubes) and/or adding mechanical damping to the tubes. The final designer-owner decision was to realize the roof without any countermeasure, to monitor it and to evaluate ‘on site’ the opportunity of acting on the tubes (a case of design assisted by testing and monitoring).

3.7 CONCLUSION

According to principle of the “design assisted by testing”, contemplated by the Eurocode, the combination of tests and calculations is increasingly used. The motivations of this increasing interest-demand are various: from the sophisticated architectural shapes to the absence of corresponding reliable fluid-dynamics models, from the increasing flexibility of structures to the necessity of checking complex aeroelastic phenomena.

The paper outlined the potentiality of wind tunnel testing and the main problems encountered in their use. These aspects have to be accurately evaluated in defining the tests specifications. The use of some data analysis techniques (such as the proper orthogonal decomposition, the sensitivity analysis etc.), in keeping the essential design parameters, was presented too.

The cited tasks were presented by referring to some of the recent experiences, made by the Authors within the design stage of steel structures: a cable stayed bridge on the Adige river (on the A31 motorway - Italy); the New Braga Stadium (Braga - Portugal); the new Unipol headquarter Tower (Bologna - Italy); the tall building and the roof on «Piazza delle Città Lombarde» (Milan - Italy); the new Bologna town-hall (Bologna - Italy).

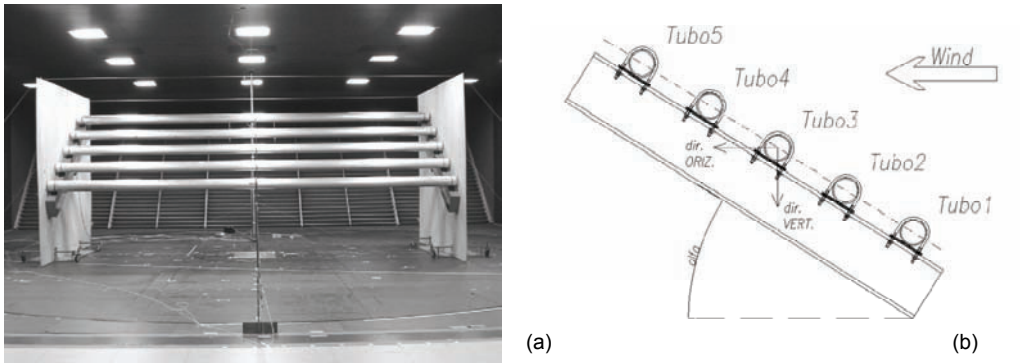
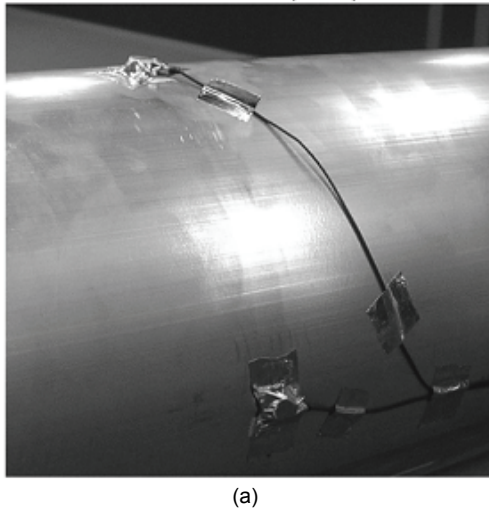
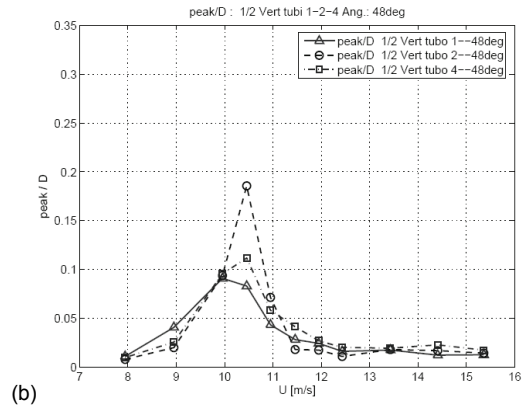


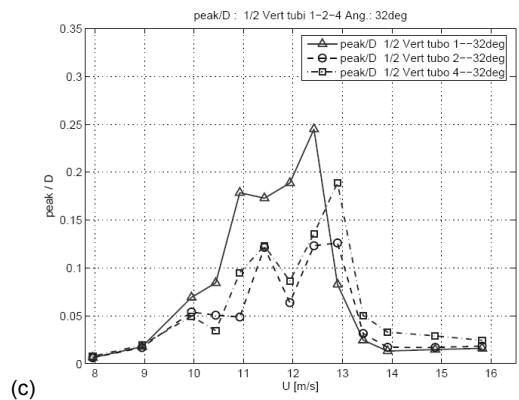
Figure 3.22 Wind tunnel model (a) and scheme (b) of one of the tube array



(a)



(b)



(c)

Figure 3.23 Accelerometers on a tube of the array (a) and vibration amplitudes (b,c) for different angles of the array setup

3.8 BASIC REFERENCES

- [1] Majowiecki M., Cosentino N., Costa C. 2007. Wind Effects and Cables Damping at the Adige Cable Stay Bridge. *Proc. IASS Symposium 2007*, Venice, Italy.
- [2] Majowiecki M., Cosentino N. 2007. Dynamic Aspects of the New Braga Stadium Large Span Roof. *Proc. IASS Symposium 2007*, Venice, Italy.

- [3] Marini M., Cosentino N., Majowiecki M. 2005. Dynamic characterization of the New Braga Stadium large span suspension roof. *Proc. International Conference on Experimental Vibration Analysis for Civil Engineering Structure EVACES*, Bordeaux, France.
- [4] Cosentino N., Majowiecki M. 2004. Analysis and mitigation of the wind induced response of large span suspended roofs: the case of the new Braga Stadium. *Proc. 8th Italian National Conference on Wind Engineering IN-VENTO*, Reggio Calabria, Italy.
- [5] Bertero R.D., Carnicer R., Puppo A.H. 2003. *Sensibility wind analysis of the roof structural system - Stadium of Braga – Portugal*. Final Report.
- [6] Puppo A.H., Bertero R.D. 1992. Evaluation of Probabilities using Orientated Simulation. *J. Struct. Eng.* 118(6), 1683-1704.
- [7] Diana G., Bocciolone M., Collina A., Tosi A., Rocchi D. 2003. *Wind tunnel investigation on Braga Stadium*. Journal Final Report.
- [8] Borri C., Bartoli G., Procino L. 2007. *Edificio a torre di via Larga (Unipol): prove in galleria del vento per la determinazione delle pressioni sulle facciate e delle forze globali al suolo*. Rapporto finale.
- [9] Quiroga P. 2005. *A study of wind effects for Milan Lombardi Government Center*. Report BLWT-SS21-2005.
- [10] Diana G. 2005. *Comune di Bologna - Sede dei Servizi Unificati - Prove in galleria del vento su modello in scala 1:50 dell'intero complesso*. Report 0202.PM.RC-F.001.001.
- [11] Diana G. 2005. *Comune di Bologna - Sede dei Servizi Unificati - Prove in galleria del vento su un modello in scala 1:1*. Report 0202.PM.RC-F.002.001.